ISSN NO: 2770-4491
Date of Publication:26-07-2023

Analysis of Reinforced Concrete Beam Elements Impregnated with Ultra-High-Performance Fibers

Inas M. Ahmed*
Email: inas.mahmood@ntu.edu.iq
Kamalaldin F. Hasan*
Email: dr_kamal@ntu.edu.iq
Maha A. Meteab*
Email: mahaadnan3@ntu.edu.iq
Arzu M. Hadi*
Email: arzuhadi@ntu.edu.iq
Qais F. Hasan*
Email: dr.qaishasan@ntu.edu.iq

Abstract: The manner of seismic elements made of Ultra-High Performance Fiber Reinforced Concrete (UHPFRC) differs significantly from conventional concrete. However, limited research exists in the literature on the dynamic manner of UHPFRC seismic members due to their high cost. Limited element programs can reduce the need for experimental studies to develop design procedures for large-scale seismic elements. Validated analytical models can be utilised to investigate the impact of geometric changes, loading schemes, and reinforcement ratios on the seismic behaviour. This research employed a limited element program, specifically ABAQUS, to model a UHPFRC beam subjected to dynamic loading and evaluate the predictive accuracy of the numerical model. The material model parameters were determined based on uniaxial pressure and tensile tests. The findings from the numerical models demonstrate that the analytical model effectively predicts the dynamic behaviour of UHPFRC beams.

Keywords: Limited element analysis, impact, UHPFRC, ABAQUS.

1. Introduction

Ultra High Performance Fiber Concrete (UYPLB) (Unknown Yield Point Low Bond) emerged as a new composite building material; steel, synthetic, etc. This composite material has good ductility, fatigue resistance, and fracture toughness. It is reinforced with fibers, with characteristic compressive strength of 150-250 MPa and tensile strength of around 10-15 MPa [1-4]. These superior properties are provided by the low water/cement ratio (approximately 2%), very fine additives that maximize grain density and provide homogeneity, steam curing and the contribution of micro steel fibers [5]. In addition to these properties of UYPLB, it can be a suitable material for reinforced concrete structures that may be exposed to dynamic loading such as nuclear power plants, military structures, transportation infrastructure, coastal structures, due to its high resistance to sudden or repeated loadings [1]. However, there is a limited number of studies in the literature on the dynamic behavior of UYPLB reinforced concrete elements. In a related study, UYPLB dynamic behavior of the beam was investigated experimentally and reported that bending fracture occurred in the beam without stirrup reinforcement [1]. In another research [6], the effect of concrete type, fiber content, and stiffening ratio on the dynamic behavior of UYPLB panels was studied experimentally. It was observed that the increase in fiber content and reinforcement ratio resulted in fewer peaks and permanent displacements under the same dynamic load. A research [7] has studied the effect of the reinforcement ratio on the bending behavior of UYPLB beams under dynamic loading. It is determined that as the reinforcement ratio increases, less permanent displacement occurs and the maximum crack width decreases. In other research [8], it was proved that if 2% of the volume of steel fibers was used in UYPLB beams under dynamic loading, the level of damage decreases and thus the permanent and maximum displacements reported that there was a significant decrease in their values. In the literature, it is seen that there are a limited number of studies examining the behavior of seismic elements produced with UYPLB under impact loads. Reasons such as not knowing the design procedure of such temple elements very well and the high

ISSN NO: 2770-4491
Date of Publication:26-07-2023

cost of the test equipment and materials to be used for the experimental study may also lead to this result. However, rapidly developing computer technologies allow such experiments to be carried out in the computer environment, and the rapid evaluation of the created test matrices with 2 or 3 dimensional models [8].

This study aims to model a reinforced concrete beam produced with UYPLB with the limited element program ABAQUS and to show that its behavior under impact loads, which is simulated realistically. The limited element program ABAQUS can perform nonlinear analysis; therefore it is used in this study. Within the scope of this study, a limited element model of a reinforced concrete beam produced with UYPLB selected from the literature was created, the modeling parameters necessary for the creation of the numerical model were explained in details, and dynamic analyses of this beam under the impact of seismic condition were made. The limited element analysis results were compared with the experimental data and results available in literature, and it was shown that the model could realistically simulate the behavior of a reinforced concrete beam under consideration [9].

2. Experimental Study

The experimental study, whose numerical analysis was performed, was selected from the literature and is related to the examination of the impact resistance of UYPLB beams with different fiber content [8]. The dimensions of the test specimens were 150 x 220 mm and their length was 2500 mm. Longitudinal reinforcements with a diameter of D16 (15.9mm) in the tension zone and D10 (9.53mm) in the compression zone were used, with D10@80 mm c/c stirrups along the beam length. In the experimental sample modelled in this study, 13 mm smooth steel fiber with an aspect ratio of 65 was used to produce UYPLB. Impact tests were carried out by freely dropping 510 kg masses to the midpoints of the test specimens from 2 different heights (0.90 and 1.15 m). The strength obtained from the uniaxial compression test for the UYPLB used in the production of the simulated beam is 211.8 MPa. The mechanical properties of reinforcement bars obtained from the results are given in Table 1.

Table 1. Physical characteristics of the reinforcement [8]

Reinforcement	Name	Diameter (mm)	E_s (GPa)	f_y (MPa)	ε_y	f_u (MPa)	ε_u
Longitudinal	D. (16)	15.899	200	509.88	0.0027	625.79	0.192
Stirrup	D. (10)	9.589	200	490.79	0.0026	608.88	0.211

3. Numerical Analysis

Numerical analysis of samples under impact of seismic loads using ABAQUS is made using the limited element program. For nonlinear dynamic analysis, open (explicit) or implicit direct integration system can be used in ABAQUS program. Faster and more efficient in solving nonlinear equations, short-term problems, the open dynamic analysis method was used in this study [9].

3.1. Loading application

The supports were defined linearly at the positions given in the experiment and their movements in the X-direction and their rotations in the Z-direction were freed according to the test data. Assuming that the steel impact weight is rigid, the object is modelled as a rigid body, and it reaches the reference point determined at the midpoint of the specimen. Movement of the impact mass only in the direction normal to the plane of the beam is to be limited. The velocity at the time of impact obtained from the experimental data was defined to the mass and the mass was positioned close to the beam surface at the initial stage of analysis. The contact between the impact load and the beam is defined using the “general contact interaction” feature, with "hard contact" feature for contact interaction [8].

3.2. Limited element geometry

Concrete in the beam mesh is modelled as a limited brick element (C3D8R) with 3 displacement degrees of freedom, 8-nodes and reduced integration points. Reinforcing bars, on the other hand, are modelled as single

ISSN NO: 2770-4491
Date of Publication:26-07-2023

degree of freedom, 2-node, linear (T3D2) limited element works in the axial direction. Concrete and reinforcement interactions are described by its embedded feature, which provides movement with a common degree of freedom between sections [10].

3.3. Materials Modeling

The elastoplastic material model was used to define the reinforcement material model. The necessary parameters to define this behavior feature were obtained from the experimental study, and are presented in Table 1. There are two basic failure mechanisms to describe the concrete material pattern: tensile cracking and compression crushing (Fig. 1). To describe the nonlinear behavior of concrete, the concrete damage plasticity model (BHP) was used. The BHP model is primarily used to analyse concrete structures under cyclic or dynamic loading [9]. As can be seen in Figure 1, the behavior of the BHP model through uniaxial tension is defined by the linear elastic relationship for the stress-strain until it reaches the maximum tensile stress value. Tensile cracking occurs in concrete reaching this stress value, the part where the strength starts to decrease with the progression of the cracks. It is defined as its stiffness and can be expressed as a decreasing stress-strain relationship or fracture energy [10]. Under uniaxial compressive loading, the BHP model exhibits a linear behavior up to σ_{co}. After this strength is exceeded, plastic deformations begin in the concrete. The behavior between σ_{c0} and σ_{cu} is expressed as strength hardening, and the behavior after exceeding σ_{cu} is called strength softening.

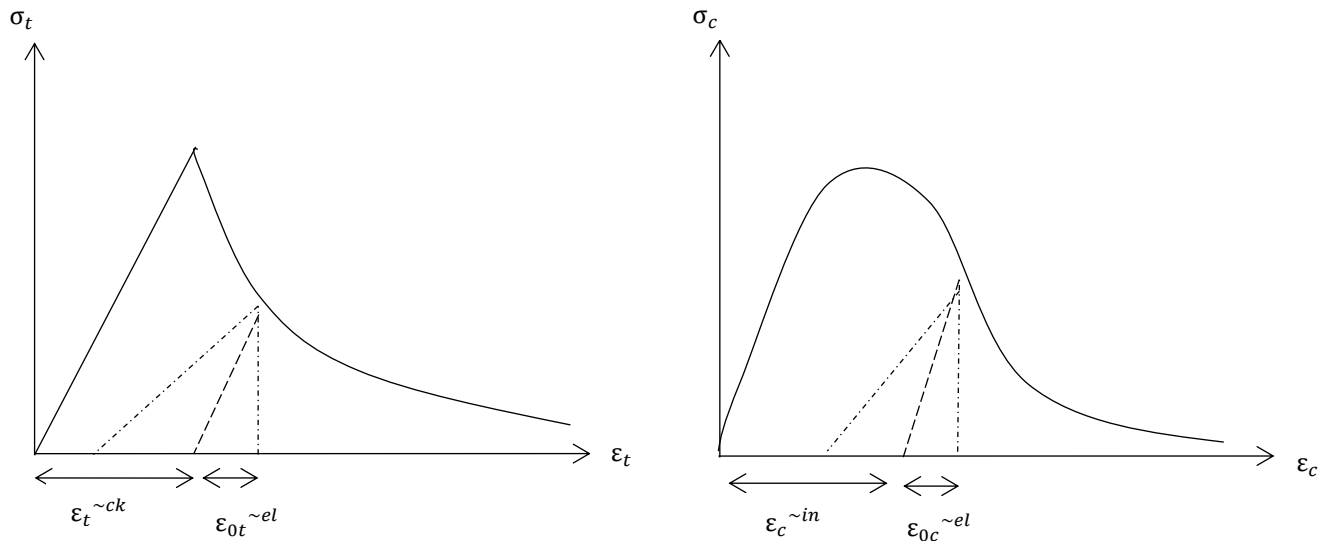

(a) Under axial tension (b) Under axial compression

Figure 1. Behavior of concrete under axial tension and compression [9]

d_c and d_t are damage parameters that express the decrease in elastic stiffness of concrete under the effect of compression and tension and are expressed by Equations 1 and 2 [11]. The damage parameter takes values ranging from 0 to 1, where 0 means no damage and 1 means totally damaged [18].

$$d_c = 1 - \frac{\sigma_c/E_0}{\sigma_c/E_0 + \varepsilon_c^{in}(1-bc)} \quad (1)$$

$$d_t = 1 - \frac{\sigma_{t0}/E_0}{\sigma_{t0}/E_0 + \varepsilon_c^{ck}(1-bt)} \quad (2)$$

To determine the power depletion envelope of the BHP model, 4 parameters are required. The eccentric parameter (ε) is assumed to be 0.1 as the default value. Typical values for the ratio of biaxial initial compressive yield stress to uniaxial initial compressive stress (σ_{bo}/σ_{co}) range between 1.10 to 1.16 [12]. This

ISSN NO: 2770-4491
Date of Publication:26-07-2023

value has been reported as 1.05 for UYPLB [13]. The K_c value was accepted as 2/3, which was given as the default value in the numerical analysis. The dilation angle (ψ) was determined by sensitivity analysis. The stress-strain behavior of concrete subjected to compression can be characterized by empirical equations derived from experimental tests [14]. Singh modified Lu's empirical equation to describe the stress-strain behavior of UYPLB under uniaxial compression [15]. Singh's formula was then applied in the finite element analysis of a full-scale beam, and its suitability for dynamic analysis was examined [9].

$$\sigma_c = f_c' \left[\frac{(E_0/E_{sc})(\varepsilon/\varepsilon_0)-(\varepsilon/\varepsilon_0)^2}{1+\left(\frac{E_0}{E_{sc}}-2\right)\left(\frac{\varepsilon}{\varepsilon_0}\right)}\right] \qquad (0 \le \varepsilon \le \varepsilon_0) \qquad (3)$$

$$\sigma_c = \frac{f_c'}{1+1/4[\{(\varepsilon/\varepsilon_0)-1\}/\{(\varepsilon_L/\varepsilon_0)-1\}]^{1.5}} \qquad (\varepsilon_0 \le \varepsilon) \qquad (4)$$

$$\varepsilon_L = \varepsilon_0 \left[\left(\frac{1.25}{10}\frac{E_0}{E_{sc}}+\frac{4}{5}\right)+\sqrt{\left(\frac{1.25}{10}\frac{E_0}{E_{sc}}+\frac{4}{5}\right)^2-\frac{4}{5}}\right] \qquad (5)$$

$$\varepsilon_0 = 750(f_c')^{0.35}x10^{-6} \qquad (6)$$

$$E_0 = 15050(f_c'/10)^{1/3} \qquad (7)$$

$$E_{sc} = f_c'/\varepsilon_0 \qquad (8)$$

where; f' is the uniaxial compressive strength of the concrete, ε is the unit strain corresponding to the value of $f'c$. E_o denotes the initial modulus of elasticity, E the secant modulus corresponding to the value of f'. Behavior of UYPLB material under tension is different. Although the rate of load reduction after fracture is very high and the deformation is very low in normal concrete, it is seen that the load after cracking increases even more in fibrous concrete. Fibers in UYPLB concrete act as a bridge, preventing the growth of micro-cracks in the concrete, and counteracting the stress released over the concrete matrix, allowing it to take some more stress until local cracks occur. Due to stress transfer, the amount of energy required for crack propagation is also normal. Behavior of normal strength concrete is much higher than concrete [16]. The idealized model approach makes the tensile behavior elastic, strain hardening and failure. It divides it into three parts as shown in Fig. 2 [2].

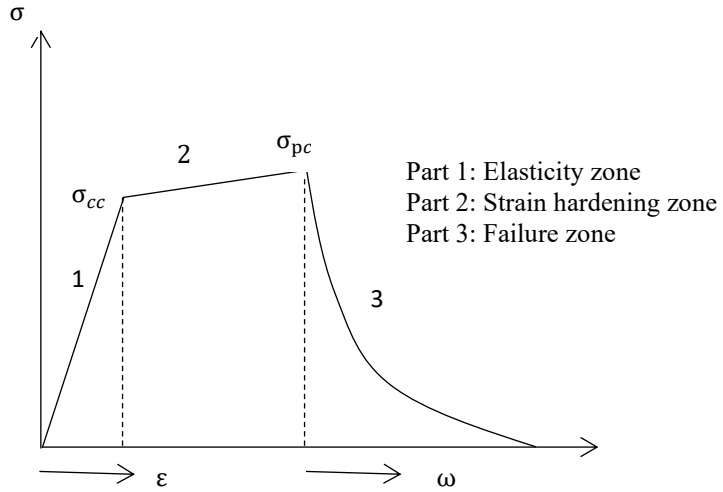

Figure 2. Idealized tensile behavior for UYPLB [2]

In the elastic part, the tensile stress-strain behavior proceeds linearly up to 90-95% of the crack strength (σ_{cc}) until it reaches the tensile strength (σ_{pc}) in the strain hardening region where microcracks and inelastic deformations occur. In the strain softening part local cracks occur and the strength starts to decrease [17]. In the experimental study, bending test was achieved to describe the tensile behavior of the concrete, and then the tensile stress-crack width graph was obtained by back analysis method, as shown in Fig. 3. For the curve modeling, the tensile stress-crack width curve obtained from the experimental study was converted into a stress-strain curve using the formulas suggested by AFGC [4], as shown in Fig. 4.

ISSN NO: 2770-4491
Date of Publication:26-07-2023

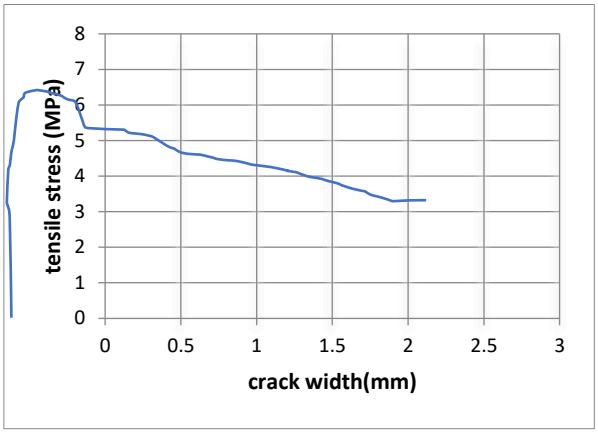

Figure 3. Crack width obtained by back analysis method [9]

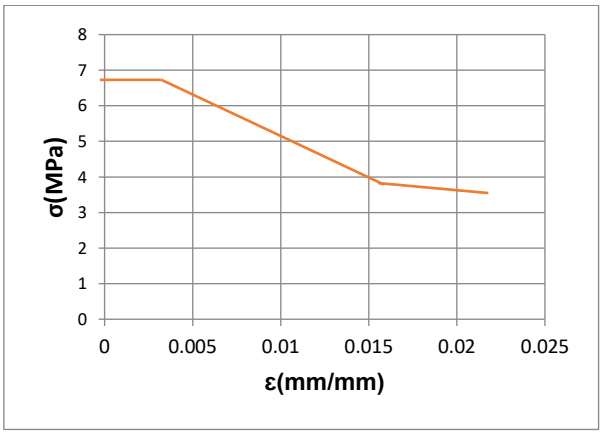

Figure 4. σ-ε curve idealized according to AFGC [4]

$$\varepsilon_{0.3} = \frac{w_{0.3}}{l_c} + \frac{f_{tj}}{\gamma_{bf} E_c} \quad (9)$$

$$\varepsilon_{1\%} = \frac{w_{1\%}}{l_c} + \frac{f_{tj}}{\gamma_{bf} E_c} \quad (10)$$

$$\varepsilon_{lim} = \frac{lf}{4l_c} \quad (11)$$

$\varepsilon_{0.3}$ denotes the unit strain value where the crack has 0.3 mm width ($w_{0.3}$), and $\varepsilon_{1\%}$ represents the unit strain value where the crack width is 1% of the beam height ($w_{1\%}$). l_c is the characteristic length and is expressed as 2/3 of the beam height. γ_{bf} is the partial factor of safety, and E_c is the concrete elasticity modulus [18].

4. Selection of limited element model parameters

In order for the limited element model to realistically simulate the beam behavior, the necessary parameters must be accurately determined. Sensitivity analysis is performed to determine the effect of these parameters on the limited element model. In previous studies, it was stated that ε, σ_{bo}/σ_{co}, K_c values did not affect the analysis results [19]. In this study, a parametric study will be made for the mesh (limited element mesh) density and dilation angle parameter [20] and the effects of these parameters on the beam behavior is to be investigated.

5. Results and discussion

Three different mesh densities, 50, 25 and 12.5 mm, were selected to determine the mesh size effect on the results gained from the analysis of the limited element model (Fig. 5). As can be shown in the figure, the limited element model behavior is approximately the same for selected mesh densities until reaching the

ISSN NO: 2770-4491
Date of Publication:26-07-2023

peak value. In terms of permanent displacements, it was seen that the mesh density affected the behavior. Considering these results, it was decided to choose 25 mm in terms of mesh density.

While the volumetric changes in concrete up to the critical stress are determined by the Poisson ratio, plastic volumetric changes begin under pressure when the critical stress is reached [21]. This behavior is taken into account by the dilation angle parameter (ψ). In the limited element model, 3 different dilation angle values were analyzed and 100 dilation angles gave results closer to the peak value (Fig. 6). In addition to the conclusions made by Othman et al. [16] and Tayeh et al. [20], it was observed that the findings were consistent with the study conducted by Wille et al. [22].

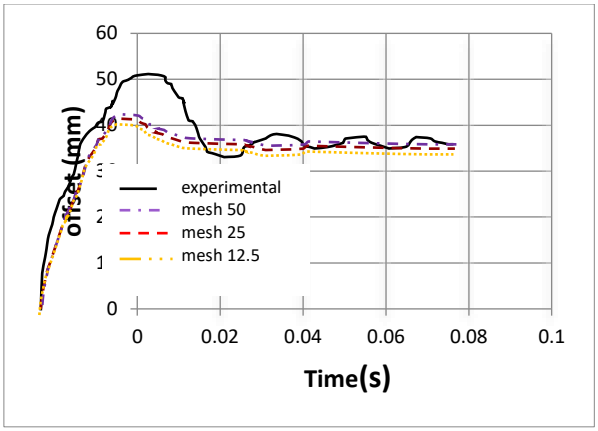

Figure 5. The effect of mesh size on the displacement-time curve

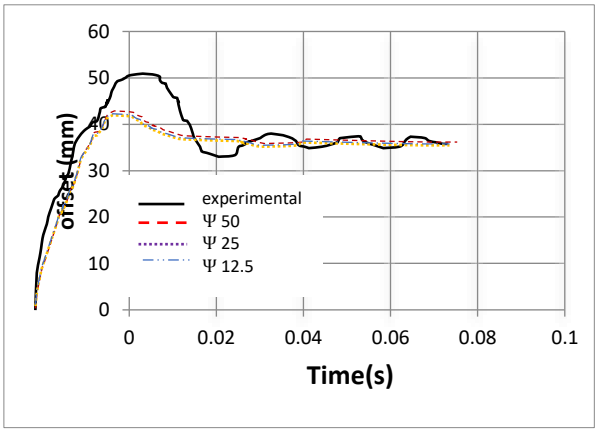

Figure 6. The effect of dilation angle parameter on the displacement-time curve

Dynamic analyses of the numerical model with the selected parameters and mesh density were made and the deformed sample is shown in Fig. 7. The results obtained by releasing the impact weight from a height of 1.15 m and 0.90 m are presented in Fig. 8 and Fig. 9, respectively. In addition, the results obtained from the experimental program and the numerical model are summarized in Table 2. As can be seen form the results obtained that the limited element models provides an acceptable agreement with laboratory experimental results. As seen, the kinetic energy values obtained for the experiments carried out by dropping loads from different heights are fully compatible with the model. The difference between the resulting deformations has maximum value of 12.15 % due to the compatibility of the boundary conditions assumptions made in the modeling with the experiment. Considering these results, in order to realistically simulate the behavior of a reinforced concrete beam produced with UYPLB under impact loads, the limited element model is suitable to be used.

ISSN NO: 2770-4491
Date of Publication:26-07-2023

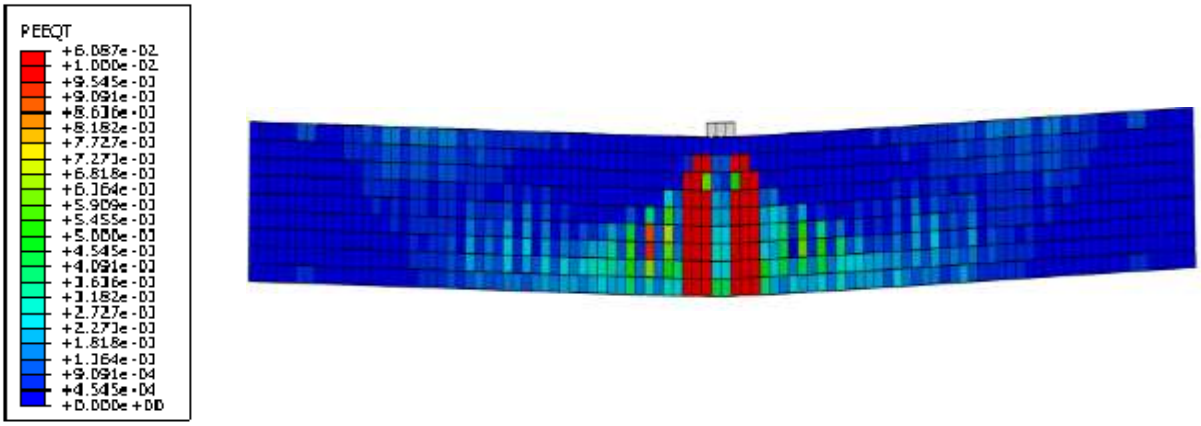

Figure 7. A typical beam deformed shape according to numerical analysis

Table 2. Comparison between the experimental and the limited element model results

Spec.	Drop height (m)		Kinetic energy (kJ)		Speed (m/s)		Maximum deformation (mm)		Permanent deformation (mm)		Fracture type	
	Exp.	Num.	Exp.	Num.	Exp.	Num.	Exp.	Num.	Exp.	Num.	Exp.	Num.
UH-S13	0.90	-	4.50	4.50	4.20	4.20	37.3	35.9	25.6	28.4	Bending	Bending
	1.15	-	5.75	5.75	4.75	4.75	51.0	44.8	37	36.9	Bending	Bending

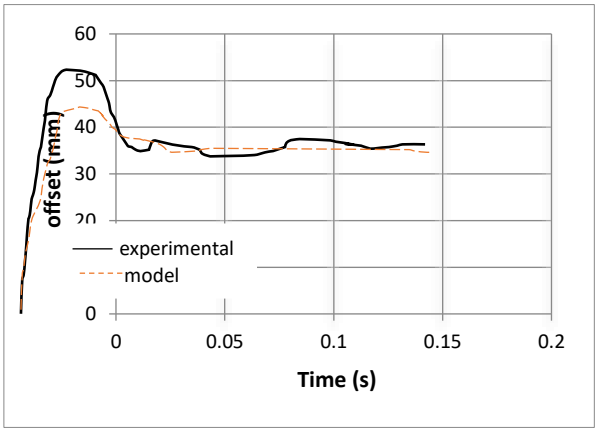

Figure 8. Displacement-time graph for 1.15 m height releasing

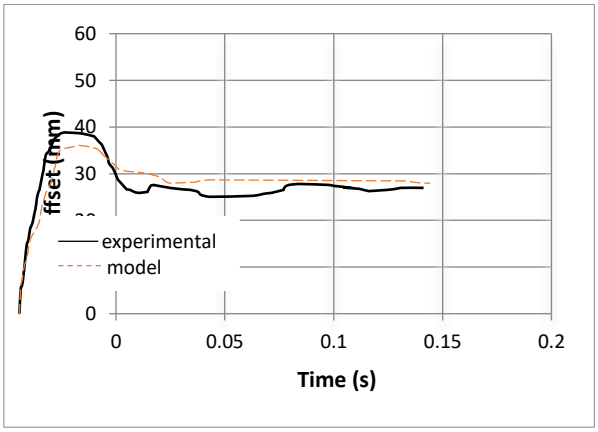

Figure 9. Displacement-time graph for 0.90 m height releasing

6. Conclusions and recommendations

According to the modeling result, the numerical simulation using the ABAQUS software gave very close results to the experimental results. Numerical analyses of UYPLB reinforced concrete beams show that the

BHP model is suitable for estimating the dynamic response of a new material, UYPLB, and the proposed concrete compression and tension curves can be used to model the behavior of high strength and fiber reinforced concretes in dynamic analysis. Limited element analysis of UYPLB reinforced concrete beams under impact loads using ABAQUS software can develop reasonable and realistic estimates to investigate possible damage modes. It is thought that the variation between the analytical model and the test results may be due to the loading speed in the material tests and the differences in the fiber orientation angle. Słomka et al. [1] stated in his study that the loading speed affects the concrete shrinkage behavior. However, the strain rate effect on the material is neglected in the model used, and this can be taken into consideration in the future. The model can be revised according to dynamic material tests.

Reference

1. Słomka-Słupik, B., Podwórny, J., Grynkiewicz-Bylina, B., Salamak, M., Bartoszek, B., Drzyzga, W., and Maksara, M., (2021). Concrete examination of 100-year-old bridge structure above the kłodnica river flowing through the agglomeration of upper silesia in gliwice: A case study. Materials, 14(4), 981.
2. Al-Osta, M.A., Isa, M.N., Baluch, M.H., and Rahman, M.K., (2017). Flexural behavior of reinforced concrete beams strengthened with ultra-high-performance fiber reinforced concrete. Construction and Building Materials, 134, 279-296.
3. Gudra, T., and Stawiski, B., (2000). Non-destructive strength characterization of concrete using surface waves. Ndt & E International, 33(1), 1-6.
4. Lu Z H, and Zhao Y G., (2021). Empirical Stress Strain Model for Unconfined High Strength Concrete under Uniaxial Compression. J. Mater. Civ. Eng., 1181-1186.
5. Othman H, and Marzouk H., (2017). Limited Element Analysis of UHPFRC Plates under Impact Loads. AFGC-ACI-fib-RILEM Int. Symposium on Ultra-High Performance Fibre-Reinforced Concrete,UHPFRC 2017, 337-346.
6. Banthia, N., Zanotti, C., and Sappakittipakorn, M., (2014). Sustainable fiber reinforced concrete for repair applications. Construction and Building Materials, 67, 405-412.
7. Chagas, Js. Nogueira, and G. Farias Moita., (2016). Fibre Reinforced Polymers in the Rehabilitation of Damaged Masonry. Sustainable Construction. Springer Singapore, 1-21.
8. Earij A., Alfano G., Cashell K., and Zhou X., (2017). Nonlinear Three-Dimensional Limited-Element modeling of Reinforced-Concrete Beams: Computational Challenges and Experimental Validation. Engineering Failure Analysis, 82, 92–115.
9. Birtel V, and Mark P, (2020). Parametericed finite element modelling of RC beam shear failure, Abaqus User's Conference 2020, 95-107.
10. Golewski, G. L., (2021). Validation of the favorable quantity of fly ash in concrete and analysis of crack propagation and its length–Using the crack tip tracking (CTT) method–In the fracture toughness examinations under Mode II, through digital image correlation. Construction and Building Materials, 296, 122362.
11. Zuki, S. S. M., Choong, K. K., Jayaprakash, J., and Shahidan, S., (2015). Effect of Diameter on Fire Exposed Concrete-Filled Double Skin Steel Tubular (CFDST) Columns under Concentric Axial Loads. Applied Mechanics and Materials, 802, 130-135.
12. Hager, I., (2013). Manner of cement concrete at high temperature. Bulletin of the Polish Academy of Sciences:Technical Sciences, 61, 145-154.
13. Dos Santos, C. C., and Rodrigues, J. P. C., (2016). Calcareous and granite aggregate concretes after fire. Journal of Building Engineering, 8, 231-242.
14. Kodur, V., (2014). Properties of concrete at elevated temperatures. ISRN Civil engineering.
15. Mazza, F., (2015). Seismic vulnerability and retrofitting by damped braces of fire-damaged r.c. framed buildings.Engineering Structures, 101, 179-192.
16. Othman H, and Marzouk H., (2016). Performance of UHPFRC Plates Under Repeated Impact Load, First International Interactive Symposium on UHPC – 2016, 1-8.

ISSN NO: 2770-4491
Date of Publication:26-07-2023

17. Singh M., Sheikh A. H., Mohamed Ali M.S., Visintin P., and Griffith M.C., (2017). Experimental and Numerical Study of The Flexural Manner of Ultra-High Performance Fibre Reinforced Concrete Beams, Construction and Building Materials 138, 12–25.
18. Baharuddin, and Nur Khaida, (2016). Evaluation of bond strength between fire-damaged normal concrete substance and ultra-high-performance fiber-reinforced concrete as a repair material. World Journal of Engineering 13(5), 461-466.
19. Słomka-Słupik, B., Podwórny, J., Grynkiewicz-Bylina, B., Salamak, M., Bartoszek, B., Drzyzga, W., and Maksara, M., (2021). Concrete examination of 100-year-old bridge structure above the kłodnica river flowing through the agglomeration of upper silesia in gliwice: A case study. Materials, 14(4), 981.
20. Tayeh, B.A., Abu Bakar, B.H., Megat Johari, M.A., and Zeyad A.M., (2014). Microtectonic analysis of the adhesion mechanism between old concrete substrate and UHPFC, Journal of Adhesion Science and Technology, 28, 1846-1864.
21. Budhe, S., (2017). An updated review of adhesively bonded joints in composite materials. International Journal of Adhesion and Adhesives, 72, 30-42.
22. Wille K., Kim D.J., and Naaman A.E., (2021). Strain Hardening UHP-FRC with low fiber contents. Materials and Structures, 44, 583–598.